Numerical Analysis of Combustion for Droplet of Hydrazine

*Mikiro Motoe**
** The Japan Aerospace Exploration Agency*
3-1-1 Yoshinodai, Chuuou, Sagamihara, Kanagawa-ken, 252-2510, Japan

Abstract

Several simulations of evaporation and combustion of fuel droplet are performed as preliminary stage for the combustion simulation in the chamber of bipropellant thruster. First, the evaporation simulation without chemical reaction for single droplets of water and n-heptane are performed. Two evaporation models such as classical equilibrium and non-equilibrium Langmuir-Knudsen models are used for the simulation, and its characteristics are understudied in order to investigate the difference between two models. Then the accuracy of the numerical code using this study is confirmed by means of comparison with existing experimental result. Next, the evaporation simulation with chemical reaction for single droplets of hydrazine is performed, and the accuracy of the numerical code is confirmed by the same way. From these simulation, it is considered that the code and the scheme using this simulation have reasonable accuracy for droplet simulation with evaporation and combustion.

1. Introduction

Bipropellant thruster is a major propulsion system of spacecraft such as satellites and space probes. A propellant used for the thruster has a characteristic that they ignite when they mix each other. When these propellants are injected individually and are mixed in the combustion chamber of the thruster appropriately, they will combust without any artificial ignition. Therefore, the typical bipropellant thruster does not equip an igniter. A combination of hydrazine and dinitrogen tetraoxide or mono methyl hydrazine and dinitrogen, the former is fuel and latter is oxidizer, are usually used as the propellant of the thruster. Since the both are liquid phase, the fuel and the oxidizer is vaporized by atomization and then mixed. The atomization is conducted by means of impingement of the fuel and the oxidizer flows. The flows form a liquid film. Then the film becomes fragments from the edge of it by means of instability. Basically, the fragments are vaporized and ignite after mixing. Additionally, it is thought that part of the propellant ignite as liquid phase [1].

Because the bipropellant thruster does not equip any igniter, it has merits as simple structure and lightweight. Not using any active ignition means that the timing of the ignition many depends on an ambient in the chamber, a mixing state of the propellant and so on, and it is difficult to be predicted. Additionally, in the property of the spacecraft mounting the thruster, there are problems that are caused by pulse ignition at operations such as a combustion instability, ignition shock and thermal load to the wall of the chamber. Due to the various problems, it has been difficult to design the bipropellant thruster appropriately yet, and the designs have been conducted by using many combustion experiment and empirical rules.

In order to improve such situations, the numerical fluid simulation have been applying to prediction of thermal load to the wall of the chamber and investigation of inner state of it [2] [3].

As baseline study of an analysis in the chamber of bipropellant thruster, the object of this study is to determine combustion property of the droplet of hydrazine in ambient of oxidizer for various cases by the combustion simulation with detailed chemical reaction model of Daimon et al. [2]. By means of this study, it can be expected to obtain valuable knowledge so that whole region of the bipropellant thruster will be analysed.

Copyright © 2015 by First Author and Second Author. Published by the EUCASS association with permission.

2 Dominant equations

2.1 Gaseous phase

In this study the gaseous phase is described by Eulerian method, and droplets are described by Lagrangian method. Dominant equations of gaseous phase, which are partially discretized at source term, are shown below.

$$\frac{\partial \rho}{\partial t}+\frac{\partial u_i}{\partial x_i}=\frac{1}{V}\sum_{k=1}^{n_d}\dot{m}_{d_k} \tag{1}$$

$$\frac{\partial \rho u_i}{\partial t}+\frac{\partial \rho u_i u_j}{\partial x_j}=-\frac{\partial p}{\partial x_i}+\frac{\partial \tau_{ij}}{\partial x_j}+\frac{1}{V}\sum_{k=1}^{n_d}F_{d_{i_k}} \tag{2}$$

$$\frac{\partial \rho e}{\partial t}+\frac{\partial \rho u_j H}{\partial x_j}=\frac{\partial}{\partial x_j}\left(u_i\tau_{ij}-q_j\right)+\frac{1}{V}\sum_{k=1}^{n_d}q_{d_{i_k}} \tag{3}$$

$$\frac{\partial \rho Y_n}{\partial t}+\frac{\partial \rho u_j Y_n}{\partial x_j}=\frac{\partial}{\partial x_j}\left(\rho D_n\frac{\partial Y_n}{\partial x_j}\right)+\frac{1}{V}\sum_{k=1}^{n_p}\dot{m}_{d_{n_k}} \tag{4}$$

$$\tau_{ij}=\mu\left(\frac{\partial u_j}{\partial x_i}+\frac{\partial u_i}{\partial x_j}-\frac{2}{3}\frac{\partial u_k}{\partial x_k}\delta_{ij}\right) \tag{5}$$

$$q_j=-\kappa\frac{\partial T}{\partial x_j} \tag{6}$$

In Eq. (1) to (6), t, x_i, ρ, u_i, p, e, H, T, Y_n , τ_{ij}, q_i , μ, κ, D_n and δ_{ij} are time, Cartesian coordinate, density, velocity, pressure, total energy per unit mass, total enthalpy, temperature, mass fraction of chemical species, viscous stress tensor, heat flux, viscous coefficient, thermal conductivity, diffusion coefficient of a chemical species and Kronecker delta respectively. The *"i, j, k"* are index of tensor, "*n*" is index of chemical species, "n_d" is droplet number included in a cell. Additionally, $\dot{m}_{d_k}$, $F_{d_{i_k}}$ and $q_{d_{i_k}}$ are influence of mass, momentum and energy from droplets in a cell, respectively.

2.2 Movement of droplet

The movement of droplets are calculated by means of PSI-Cell method [4], and the dominant equations of single droplet are shown in Eq. (7) to (10).

$$\frac{dU_{d_i}}{dt}=F_{d_i} \tag{7}$$

$$F_{d_i}=\frac{\pi}{8}C_D\rho d_d^2\left|u_i-U_{p_i}\right|\left(u_i-U_{d_i}\right) \tag{8}$$

$$C_D=\frac{24}{Re_d}\left(1+0.15Re_d^{0.687}\right) \tag{9}$$

$$Re_d=\frac{\rho d_d\sqrt{\left(u_i-U_{d_i}\right)^2}}{\mu} \tag{10}$$

Then, U_{d_i}, C_D, d_d and Re_d are velocity of droplet, drag coefficient of droplet, diameter of droplet and Reynolds number based on relative velocity of gas and droplet and the diameter, respectively.

2.3 Evaporation of droplet

In this study, the classic model [5] and the non-equilibrium model Langmuir-Knudsen [6] [7] are performed for evaporation of a droplet. Formulations of the classic model are shown in Eq. (11) to (17).

$$\frac{dm_d}{dt} = -A_d N_{sd} \tag{11}$$

$$N_{sd} = k_c (C_{sd,s} - C_{sd,\infty}) \tag{12}$$

$$k_c = \frac{D_{sd,m}}{d_d} \left(2.0 + 0.6 {Re_d}^{1/2} Sc^{1/3}\right) \tag{13}$$

$$C_{sd,\infty} = X_{sd} \frac{p_\infty}{R_0 T_\infty} MW_{sd} \tag{14}$$

$$C_{sd,s} = \frac{P_{sat}}{R_0 T_d} MW_{sd} \tag{15}$$

$$P_{sat} = P_0\, exp \left\{ \frac{L}{R_0 / MW_{sd}} \left(\frac{1}{T_0} - \frac{1}{T_d} \right) \right\} \tag{16}$$

$$L = ln \left(\frac{P_1}{P_0} \right) \frac{R_0\ / MW_{sd}}{\left(\frac{1}{T_0} - \frac{1}{T_1} \right)} \tag{17}$$

Then, m_d, A_d, N_{sd}, k_c, $D_{sd,m}$, Sc, $C_{sd,s}$, $C_{sd,\infty}$, X_{sd}, p_∞, T_∞, R_0, MW_{sd}, P_{sat}, T_d and L are the mass of droplet, the surface area of droplet, the vapor mass flux of droplet, the mass transfer coefficient, the mass diffusion coefficient between mixture gas and vapor of droplet, Schmidt number, the vapor concentration at droplet surface, the vapor concentration at mixture gas, the mole fraction of species of vapor, the pressure of mixture gas, the temperature of mixture gas, the universal gas constant, the molecular weight of droplet component, the saturated vapor pressure, the droplet temperature and the latent heat, respectively. P_0, T_0, P_1 and T_1 are the reference pressure and temperature. Index “sd” means the component of chemical species of droplet.
Formulations of the non-equilibrium model are shown in Eq. (18) to (25).

$$\frac{dm_d}{dt} = -\frac{Sh}{3Sc} \left(\frac{m_d}{\tau_d} \right) H_M \tag{18}$$

$$\tau_d = \frac{\rho_d d_d^2}{18\mu} \tag{19}$$

$$H_M = ln[1 + B_{M,neq}] \tag{20}$$

$$B_{M,neq} = \frac{Y_{s,neq} - Y_{sd,\infty}}{1 - Y_{s,neq}} \tag{21}$$

$$Y_{s,neq} = \frac{X_{s,neq}}{X_{s,neq} + \left(1 - X_{s,neq}\right) MW_{mix}\ / \ MW_{sd}} \tag{22}$$

$$X_{s,neq} = \frac{P_{sat}}{p_\infty} - \left(\frac{L_K}{d_d / 2} \right) \beta \tag{23}$$

$$L_K = \frac{\mu \sqrt{2\pi T_d R_0 MW_{sd}}}{Sc\ p_\infty} \tag{24}$$

$$\beta = -\left(\frac{3Pr\tau_d}{2} \right) \frac{\dot{m}_d}{m_d} \tag{25}$$

Then, τ_d, H_M, ρ_d, $B_{M,neq}$, $Y_{s,neq}$, $Y_{sd,\infty}$, $X_{s,neq}$, MW_{mix}, L_K and β are the droplet time constant, the specific driving potential for mass transfer, the density of droplet, non-equilibrium Spalding transfer number for mass, the non-equilibrium vapor surface mass fraction, the mass fraction of species of vapor in mixture gas, the non-equilibrium vapor surface mole fraction, the molecular weight of mixture gas, the Knudsen layer thickness and the non-dimensional evaporation parameter, respectively.

2.4 Heat transfer of droplet

A Formulation of heat tranfer between droplet and gas which are performed with the classical model are shown below.

$$m_d C_L \frac{dT_d}{dt} = hA_p (T_\infty - T_d) + L \frac{dm_d}{dt} \tag{26}$$

In Eq. (26), C_L and h are the specific heat of droplet and heat transfer coefficient between droplet and mixture gas, respectively.

A Formulation of heat tranfer which are performed with the non-equilibrium model are shown below.

$$\frac{dT_d}{dt} = \frac{Nu}{3Pr}\frac{\beta}{e^{\beta}-1}\left(\frac{C_p\ /\ C_L}{\tau_d}\right)(T_\infty - T_d) + \left(\frac{L_V}{C_L}\right)\frac{\dot{m}_d}{m_d} \tag{27}$$

In Eq. (27), Nu and C_p are Nusselt number and specific heat of mixture gas, respectively.

2.5 Chemical reaction of hydrazine

Chemacal reaction of hydrazine is calcurated by means of detailed chemical reaction model of Daimon et al. [2]. This model has 39 chemical spesies and 261 reactions.

3. Numerical methods

The numerical code employed here is “LS-Flow”: JAXA’s in-house, unstructured finite volume method, compressible Navier-Stokes solver for arbitrary polygons/polyhedral [8]. The numerical flux is calculated by means of SLAU scheme of Shima et al. [9], and the values of interface are interpolated by 2nd order MUSCL scheme with Venkatakrishnan limiter. The time integration of gaseous phase is performed by means of 2nd order LU-SGS scheme with inner iteration. The time integration of chemical reaction is separated from that of gaseous phase, and is performed by means of ERENA method of Morii et al. [10] which based on explicit time integration scheme.

4. Analysis object

As a preliminary analysis, two examinations of evaporation of single droplet which one is water and the other is n-heptane are simulated in order to validate the numerical code. The examination of water droplet is performed by Kobayashi [11]. A single droplet is suspended by slight fiber of quarts in the oven filled by high temperature static air as shown in figure 1, and the time series of diameters of the drop let are measured. The examination of n-heptane droplet is performed by Hiroyasu et al. [12]. The droplet is suspended by slight quarts fiber with spherical point in the pressure vessel which is filled by nitrogen as shown in figure 2, and the temperature and the pressure in the chamber can be varied. As same as the examination of water, the time series of diameters of the drop let are measured.

Subsequently, the simulation of hydrazine droplet with chemical reaction is performed, and it is based on an examination of Alison [13]. As shown in Fig. 3, in the simulation a hydrazine droplet is suspended by quarts fiber in burned gas flow with high temperature, and the hydrazine will causes autolysis reaction. Time series of the droplet diameters are measured, and the mass burning rates $\dot{M}$ are calculated by means of Eq. (28) using the gradient of the time series K(Eq. (29)).

In this study, the simulations are performed for several cases of above examinations as shown in Table 1, and the initial droplet temperatures are determined 300 [K] arbitrarily because the references do not mention about it.

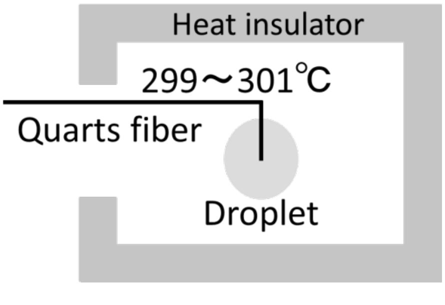

Figure 1: The examination of water droplet

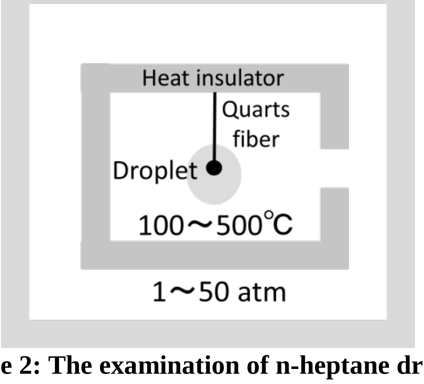

Figure 2: The examination of n-heptane droplet

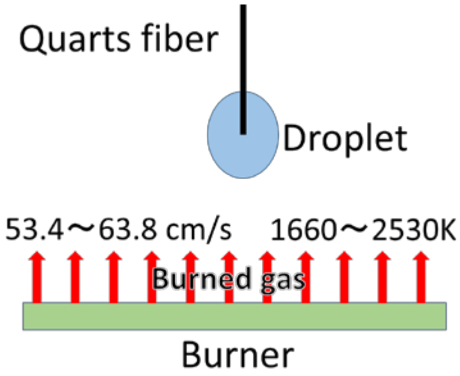

Figure 3: The examination of hydrazine droplet

$$\dot{M} = \frac{1}{4}\pi K \rho_d d_d \tag{28}$$

$$K = \frac{d\, d_d^2}{ds} \tag{29}$$

Table 1: The simulation condition

	Water droplet	N-heptane droplet	Hydrazine droplet
Initial droplet diameter [mm]	1.38	1.8	1.3
Initial droplet temperature [K]	300	300	300
Ambient temperature [K]	572	773	2060
Ambient pressure [atm]	1	1	1
Free stream velocity [m/s]	0	0	0.0557

5. Numerical setup

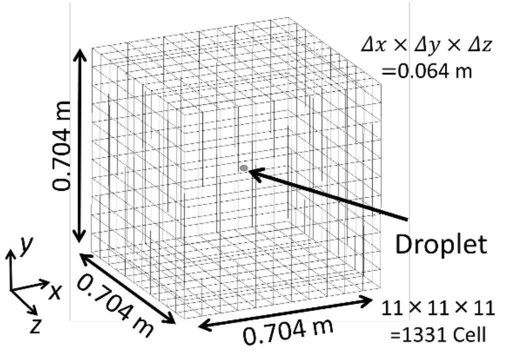

Figure 4: Numerical grid for water and n-heptane droplet

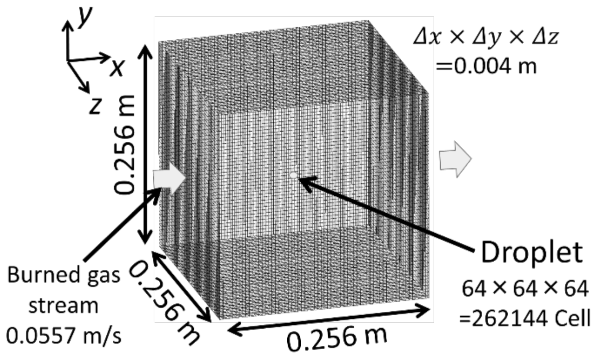

Figure 5: Numerical grid for hydrazine grid

Figure 4 shows numerical grid used for the simulations of water and n-heptane droplet evaporation. As shown in the figure, the grid is a 0.704 [m] cube which is divided equal 11 intervals on a side, therefore the number of cell is 1331, and the grid space is 0.064 [m]. The droplet is sated at the canter of the grid, and quarts fiber and other equipment are not concerned. The time step of calculation for water droplet is 2×10^{-6} [s], and for n-heptane droplet is 1×10^{-6} [s]. The boundary-condition that pressure and temperature are fixed in the ambient value as shown in the Table 1 is common in all boundary. These simulations are performed by a work station which has two Intel® Xeon® E5-2640 six core CPU, divided into 12 areas and parallelized by MPI.

Figure 5 shows numerical grid used for the simulations of hydrazine droplet evaporation. As shown in the figure, the grid is a 0.256 [m] cube which is divided equal 64 intervals on a side. The number of cell is 262144, and the grid space is 0.004 [m]. The droplet is sated at the canter of the grid, and quarts fiber and other equipment are not modelled similarly above. The time step of this calculation is 2×10^{-7} [s]. The free stream flow to forward x direction with the speed of 0.0557 [m/s], the pressure of 1 [atm] and the temperature of 2060 [K]. As same as former simulations, the boundary-condition that velocity, pressure and temperature are fixed in the free stream condition is common in all boundary. The simulations are performed on JAXA Supercomputer System generation 2 (JSS2), divided into 995 areas and parallelized by MPI.

6. Results

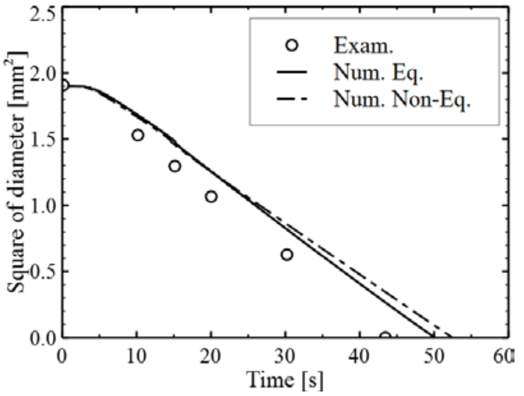

Figure 6: Distribution of square of diameter of water

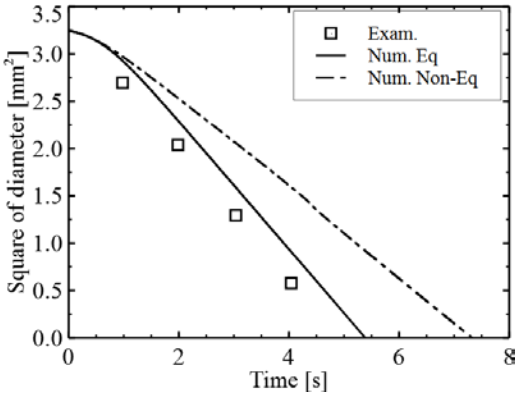

Figure 7: Distribution of square diameter of n-heptane

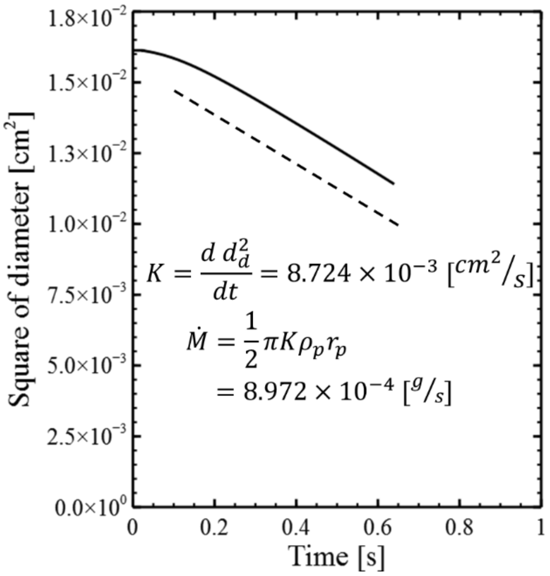

Figure 8: Distribution of square of diameter of hydrazine

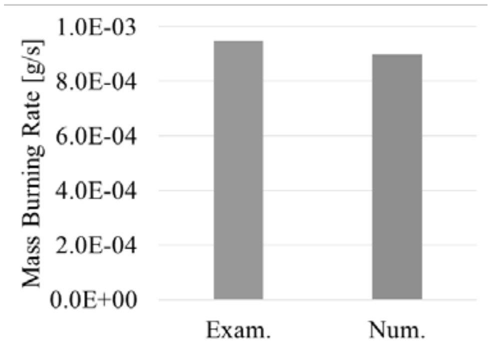

Figure 9: Comparison of mass burning rate

The results of evaporation simulations of water and n-heptane are shown in figure 6 and figure 7, respectively. The calculations are performed by using two evaporation models mentioned above. The X axis and the Y axis of these figures are time and square of diameter of droplet. From the figure 6, though it can be seen that differences of evaporation time between the two numerical results and examination result are about 10 % of examination, the slopes are well corresponding to one of examination. It can be thought that the initial droplet temperature has a lag between the examination, and it causes the difference of evaporation time. In this case, the two evaporation models indicate roughly same results. The result of non-equilibrium is longer than equilibrium one, it is because the calculated mole fraction of evaporated droplet is smaller than the one at equilibrium condition as shown in Eq. (23).

As shown in figure 7, it can be seen that the numerical result which is calculated by the equilibrium model and one of the examination are well corresponding each other, but the result of non-equilibrium model does not correspond to the the examination. The non-equilibrium model evaluates 45 % longer evaporation time based on the equilibrium model than that of the equilibrium model. It can be considered that the reason why the non-equilibrium model evaluates such result unlike the case of water is involved in the difference of evaporation rate ($\dot{m}$) between water droplet and n-heptane droplet. The Eq. (23) and Eq. (25) indicate that the bigger evaporation rate promotes the more difference from the equilibrium model. Therefore, the difference between two models is conspicuous in the case of n-heptane which has faster evaporation rate.

From above two figures, it can be confirmed that the numerical code used in this study with the equilibrium evaporation model has satisfactory accuracy for a problem of single droplet evaporation.

Figure 8 shows time series of square of diameter of hydrazine droplet. The mass burning rate is calculate by means of Eq. (28) using the gradient of liner part of the figure. The equilibrium evaporation model is used in this simulation. Figure 9 shows the mass burning rate of the examination and the simulation. As shown in the figure, both values are well corresponding to each other, and its difference is about 6 % based on the examination. Therefore, it can be thought that the numerical code employed here has the sufficient precision for evaporation problem of hydrazine droplet with chemical reaction.

7. Summary

First the evaporation simulation without chemical reaction for single droplets of water and n-heptane are performed. The two evaporations model such as the equilibrium and the non-equilibrium model are compared with existing experimental result, and it is confirmed that the equilibrium model shows sufficient result. Next, the evaporation simulation with chemical reaction for single droplets of hydrazine are performed, and the accuracy of the numerical code is confirmed by the same way. From these simulation, it is considered that the code has reasonable accuracy for droplet simulation with evaporation and combustion.

References

[1] W. Daimon, Y. Gotoh and I. Kimura, "Mechanism of Explosion Induced by Contact of Hypergolic Liquids," *Journal of Propulsion and Power,* vol. 7, no. 6, pp. 946-952, 1991.

[2] Y. Daimon, H. Terashima and M. Koshi, "Chemical Kinetics of Hypergolic Ignition in N2H4/N2O4-NO2 Gas Mixtures," *Journal of Propulsion and Power,* vol. 30, no. 3, pp. 707-716, 2014.

[3] H. Tani, H. Terashima, M. Kosh and Y. Daimon, "Hypergolic ignition and flame structures of hydrazine/nitrogen tetroxide co-flowing plane jets," *Proceedings of the Combustion Institute,* vol. 35, no. 2, pp. 2199-2206, 2015.

[4] C. T. Crowe, M. P. Sharma and D. E. Stock, “The Particle-Source-In Cell (PSI-CELL) Model for Gas-Droplet Flows,” *Journal of Fluids Engineering,* vol. 99, no. 2, pp. 325-332, 1977.

[5] G. A. Godsave, "Studies of the combustion of drops in a fuel spray - the burning of single drops of fuel," *Fourth Symposium (International) on Combustion,* vol. 4, no. 1, pp. 818-830, 1953.

[6] J. Bellan and K. Harstad, "Analysis of the convective evaporation of nondilute clusters of drops," *International Journal of Heat and Mass Transfer,* vol. 30, no. 1, pp. 125-136, 1987.

[7] R. Miller, K. Harstad and J. Bellan, "Evaluation of equilibrium and non-equilibrium evaporation models for many-droplet gas-liquid flow simulations," *International Journal of Multiphase Flow,* vol. 24, no. 6, pp. 1025-1055, 1998.

[8] K. Fujimoto and K. Fujii, "Study on the Automated CFD Analysis tools for Conceptual Design of Space Transportation Vehicles," *5th Joint ASME/JSME Fluids Engineering Conference Proceedings, FEDSM 2007-37128,* 2007.

[9] E. Shima and K. Kitamura, "Parameter-Free Simple Low-Dissipation AUSM-Family Scheme for All Speeds," *AIAA JOURNAL,* vol. 49, no. 8, pp. 1963-1709, 2011.

[10] Y. Morii, H. Terashima, M. Koshi, T. Shimizu and E. Shima, "Fast and robust time integration method for stiff chemical kinetic ODEs," *AIAA 2014-3920,* 2014.

[11] K. Kobayasi, "A Study on the Evaporation and Combustion of a Single Droplet : 1st Report : Surface Temperature of Evaporating Droplet and its Measurement," *Transactions of the Japan Society of Mechanical Engineers,* vol. 20, no. 100, pp. 831-837, 1954.

[12] H. Hiroyasu, T. Kadota and T. Senda, "Evaporation of a Single Droplet at Elevated Pressures and Temperatures : Part 1, Experimental Study," *Transactions of the Japan Society of Mechanical Engineers,* vol. 40, no. 339, pp. 3147-3154, 1974.

[13] B. C. Allison, “Hybrid and Decomposition Combustion of the Hydrazine Fuels,” *NASA CR-72977,* 1971.